
Cross-modal Active Complementary Learning with Self-refining Correspondence

Yang Qin¹, Yuan Sun¹, Dezhong Peng^{1,3,4}, Joey Tianyi Zhou²,
Xi Peng¹, Peng Hu^{1*}

¹ College of Computer Science, Sichuan University, Chengdu, China.

² Centre for Frontier AI Research (CFAR) and Institute of High
Performance Computing (IHPC), A*STAR, Singapore.

³ Chengdu Ruibei Yingte Information Technology Co., Ltd, Chengdu, China.

⁴ Sichuan Zhiqian Technology Co., Ltd, Chengdu, China.

{qinyang.gm, joey.tianyi.zhou, pengx.gm, penghu.ml}@gmail.com,
sunyuan_work@163.com, pengdz@scu.edu.cn

Abstract

Recently, image-text matching has attracted more and more attention from academia and industry, which is fundamental to understanding the latent correspondence across visual and textual modalities. However, most existing methods implicitly assume the training pairs are well-aligned while ignoring the ubiquitous annotation noise, *a.k.a* noisy correspondence (NC), thereby inevitably leading to a performance drop. Although some methods attempt to address such noise, they still face two challenging problems: excessive memorizing/overfitting and unreliable correction for NC, especially under high noise. To address the two problems, we propose a generalized Cross-modal Robust Complementary Learning framework (CRCL), which benefits from a novel Active Complementary Loss (ACL) and an efficient Self-refining Correspondence Correction (SCC) to improve the robustness of existing methods. Specifically, ACL exploits active and complementary learning losses to reduce the risk of providing erroneous supervision, leading to theoretically and experimentally demonstrated robustness against NC. SCC utilizes multiple self-refining processes with momentum correction to enlarge the receptive field for correcting correspondences, thereby alleviating error accumulation and achieving accurate and stable corrections. We carry out extensive experiments on three image-text benchmarks, *i.e.*, Flickr30K, MS-COCO, and CC152K, to verify the superior robustness of our CRCL against synthetic and real-world noisy correspondences. Code is available at <https://github.com/QinYang79/CRCL>.

1 Introduction

Image-text matching aims to search the most relevant samples across different modalities, which is fundamental for most cross-modal tasks [1, 2, 3, 4, 5, 6]. The core of image-text matching is how to accurately measure the similarity between distinct modalities, however, which is challenging due to the visual-textual discrepancy. To tackle the challenge, numerous deep methods are presented to learn the visual-semantic associations of image-text pairs and achieve remarkable progress, thanks to the powerful representation ability of Deep Neural Networks (DNNs) and some well-designed similarity inference architectures [7, 8, 4, 9]. They could be roughly divided into two groups, *i.e.*, global-level methods [7, 9] and local-level methods [8, 4], which aim at learning the image-to-sentence and region-to-word correlation to infer the cross-modal similarity, respectively. Although these methods

*Corresponding author.

achieved promising matching performance, most of them implicitly require large-scale well-aligned data for training, which is expensive or even impossible to collect due to ubiquitous noise in real-world scenarios [10, 11]. Therefore, there is inevitably imperfect alignment lurking in the data, *i.e.*, noisy correspondence (NC) [12], resulting in inferior performance.

To handle the NC problem, some prior arts are presented to alleviate the adverse impact of NC in various tasks, *e.g.*, partially view-aligned clustering [13, 14, 15, 16], video-text retrieval [17], visible-infrared person re-identification [18], and image-text matching [12, 19, 20]. Specifically, inspired by learning with noisy labels [21, 22], some works [12, 23, 24] are proposed to alleviate the negative impact brought by NC. These works attempt to leverage the memorization effect of DNNs [25] to gradually distinguish the noisy image-text pairs for robust learning in a co-teaching manner. Furthermore, the predicted soft correspondence is used to recast a soft margin to replace the scalar margin of triplet ranking loss [7], which helps to avoid misleading the model by mismatched pairs. However, the soft-margin ranking loss is experimentally found to provide only limited robustness against NC, especially under high noise (as shown in Table 6), due to unstable division based on inaccurate predictions. In contrast, some works [19, 20] aim to enhance the robustness of cross-modal methods against NC by starting with a robust loss function, *i.e.*, avoiding over-amplification of wrong supervision information to reduce misleading risk. However, the lack of explicitly mitigating the effect of easily separable noise makes them hard to further improve the performance.

To address the aforementioned issues, we propose a generalized robust framework, dubbed CRCL, for learning with noisy correspondences. CRCL could be easily migrated into existing image-text matching methods to enhance their robustness against NC. Our framework introduces a novel Active Complementary Loss (ACL) that applies active and complementary learning to mutually boost robustness against NC. Specifically, we present a robust complementary learning loss that employs complementary pairs, such as “input image-text pairs are irrelevant”, to conduct indirect cross-modal learning with exponential normalization. Due to the low likelihood of selecting incorrect complementary pairs, robust complementary learning could reduce the risk of providing incorrect supervision and smooth the losses, thus embracing robustness against NC. However, the robust loss will face the underfitting problem, leading to suboptimal performance. To overcome this issue, a weighted Active learning loss is proposed to enforce the model focus on more reliable positive pairs in addition to only complementary pairs. In addition, we propose a Self-refining Correspondence Correction paradigm (SCC) to obtain stable and accurate correspondence correction. SCC utilizes Momentum Correction (MC) to aggregate historical predictions for stable and accurate correspondence corrections. By combining multiple Self-Refining processes (SR) throughout the entire training process, we alleviate over-memorization for NCs. In summary, the key contributions and innovations of this work are as follows:

- We propose a generalized Cross-modal Robust Contrastive Learning framework (CRCL) to address a pressing and widely-exist problem in image-text matching, *i.e.*, noisy correspondence. CRCL empowers existing methods with strong robustness through the perspectives of robust loss and correction techniques.
- A novel Active Complementary Loss (ACL) is presented to balance active and complementary learning, mutually enhancing robustness against NC while encapsulating correct cross-modal associations in the latent common space.
- We design an effective Self-refining Correspondence Correction paradigm (SCC) to achieve accurate and stable soft correspondences, which enables the prediction-based corrections to perceive larger fields and self-refine from the historically learned knowledge.
- Extensive experiments verify the effectiveness and superiority of our framework on three benchmark image-text datasets: Flickr30K, MS-COCO, and CC152K. Additionally, comprehensive ablation studies and insightful analyses demonstrate the reliability and practicability of the proposed CRCL.

2 The Proposed Method

2.1 Preliminaries and Problem Statement

To be specific, we first provide some definitions of instance-level image-text matching so as to conveniently study noisy correspondence. Let $\mathcal{D} = \{\mathcal{I}, \mathcal{T}, \mathcal{Y}\}$ be an image-text dataset, where $\mathcal{I} =$

$\{I_i\}_{i=1}^N$ and $\mathcal{T} = \{T_i\}_{i=1}^N$ are the training image and text set with size of N . The correspondence label space is defined as $\mathcal{Y} = \{y_{ij} | i = 1, \dots, N; j = 1, \dots, N\}$, where y_{ij} represents the correspondence of pair (I_i, T_j) , *i.e.*, if I_i and T_j are matched (*i.e.*, positive pair), $y_{ij} = 1$ otherwise $y_{ij} = 0$. We assume each pair with the same indices has matched correspondence, *i.e.*, $y_{ii} = 1, i = 1, \dots, N$. However, due to the ubiquitous noise during data collection, some negative pairs are mismatched as positives, *a.k.a* noisy correspondence (NC) [12, 19], which would introduce wrong supervisory information and misguide model training, leading to performance degradation. Mathematically, we define NC as shown in Definition 1.

Definition 1. *Due to the existence of NC, the learner only has access to the noisy training data (\mathcal{D}_η), instead of clean data (\mathcal{D}). Thus, the correspondence label for pair (I_i, T_j) is reconsidered as*

$$\tilde{y}_{ij} = \begin{cases} y_{ij} & \text{with probability } (1 - \eta_{ij}), \\ 1 - y_{ik} & \text{with probability } \bar{\eta}_{ik}, \forall k \neq j. \end{cases} \quad (1)$$

For all pairs, conditioned on that if $i = j$ then $y_{ij} = 1$ else $y_{ij} = 0$, we have $\sum_{j \neq k} \bar{\eta}_{ik} = \eta_{ij}$. Similar to the definitions of noisy labels [26], we assume that NC is uniform, *i.e.*, $\eta_{ij} = \eta$ and $\bar{\eta}_{ik} = \frac{\eta}{N-1}, \forall k \neq j$, where η is a constant to represent the noise rate.

The key to learning with noisy correspondence is to alleviate the misleading impact and rectify the mismatched pairs. One direct solution is to enhance the robustness of loss function \mathcal{L} against noisy pairs, which can help prevent overfitting on mismatched pairs. The second aims at using the memorization effect of DNNs [25] to discriminate the mismatched pairs, thus removing unreliable supervision from the training data.

For image-text matching, images and texts are first projected into a shared representation space by two modality-specific networks, denoted as v and g , respectively. The cross-modal similarity of a given pair (I_i, T_j) is then computed as $S(v(I_i), g(T_j))$, where $S(*)$ could be the cosine function [7, 9] or a relevance inference module [8, 4]. For brevity, $S(v(I_i), g(T_j))$ is denoted as $S(I_i, T_j)$ or S_{ij} in the following. The computed similarities could be considered as supporting evidence for retrieved results. Thus, the learning objective of image-text matching is to maximize the cross-modal similarities of positive pairs while minimizing those of negatives in the latent common space, which is commonly achieved by using contrastive learning [7, 8, 4].

The widely-used triplet ranking loss [7] has shown excellent performance in cross-modal contrastive learning tasks [7, 27]. However, recent research [19] has demonstrated that this loss function fails to perform well in image-text data with NCs, especially when using the hardest negative samples as comparison items. To address this issue, some works proposed an adaptive soft margin approach to improve the robustness of the ranking loss [12, 24, 23], which is defined as follows:

$$\mathcal{L}_{soft}(I_i, T_i) = \left[\hat{\alpha}_i - S(I_i, T_i) + S(I_i, \hat{T}_h) \right]_+ + \left[\hat{\alpha}_i - S(I_i, T_i) + S(\hat{I}_h, T_i) \right]_+, \quad (2)$$

where \hat{T}_h and \hat{I}_h denote the hardest cross-modal samples in a mini-batch, $\hat{\alpha}_i$ is a soft margin adaptively computed by $\hat{\alpha}_i = \frac{m^{\hat{y}_{ii}} - 1}{m - 1} \alpha$, α is a constant margin, m is a curve parameter, and \hat{y}_{ii} is the rectified correspondence between I_i and T_i . However, this approach has two disadvantages: 1) The margin setting α may not be consistent with the empirical setting under NC scenarios. 2) The inaccurate prediction \hat{y}_{ii} can still easily produce the risk of misleading gradient, which can cause trivial solutions to fail, especially in the case of high noise (*e.g.*, the results of NCR [12] and BiCro [23] on Flickr30K with 80% noise). To overcome these limitations, we propose a novel Active Complementary Loss (ACL) under the risk minimization theory [28, 26] to provide noise tolerance for noisy pairs while ensuring discriminative learning.

2.2 Active Complementary Loss

For the image-text dataset \mathcal{D} , our goal is to learn a cross-modal model (\mathcal{M}) that can discriminatively identify the positive (matched) and negative (unmatched) pairs well for retrieval, which is intuitively equivalent to maximizing bidirectional matching probabilities of positives. The bidirectional matching probabilities for pair (I_i, T_j) are defined as:

$$p_{ij}^\circ = f(I_i, T_j) = \frac{e^{(S_{ij}/\tau)}}{\sum_{l=1}^N e^{(S_{il}/\tau)}}, \quad p_{ji}^\circ = f(T_j, I_i) = \frac{e^{(S_{ij}/\tau)}}{\sum_{l=1}^N e^{(S_{lj}/\tau)}}, \quad (3)$$

where τ is a temperature parameter [29, 30, 31], f is regarded as the cross-modal decision function, and “ \circ , \diamond ” means the two retrieval directions, *i.e.*, image-to-text and text-to-image, respectively. For any loss function \mathcal{L} , the matching risk of f for image-text matching can be defined as

$$R_{\mathcal{L}}(f) = \mathbb{E}_{(I_i, y_i) \sim \mathcal{D}} [\mathcal{L}(f(I_i, T_i), y_i)] + \mathbb{E}_{(T_i, y_i) \sim \mathcal{D}} [\mathcal{L}(f(T_i, I_i), y_i)], \quad (4)$$

where $\mathbb{E}[\cdot]$ represents the expectation operator. Considering noisy correspondences, the risk of f in noisy data \mathcal{D}_η could be formulated as follows:

$$R_{\mathcal{L}}^\eta(f) = \mathbb{E}_{(I_i, \tilde{y}_i) \sim \mathcal{D}_\eta} [\mathcal{L}(f(I_i, T_i), \tilde{y}_i)] + \mathbb{E}_{(T_i, \tilde{y}_i) \sim \mathcal{D}_\eta} [\mathcal{L}(f(T_i, I_i), \tilde{y}_i)], \quad (5)$$

where \tilde{y}_{ij} is the noisy correspondence label as shown in Definition 1. Thus, the cross-modal learning objective is to learn a model $\mathcal{M}_{\mathcal{L}}^*$ with a global minimizer f_η^* of $R_{\mathcal{L}}^\eta(f)$. To achieve robustness, f_η^* should be also the global minimizer of $R_{\mathcal{L}}(f)$ on the noise-free data.

Inspired by complementary contrastive learning [20], we propose to optimize the matching probabilities of all negative pairs for learning with noisy data indirectly, thereby avoiding fast overfitting to NC. Simultaneously, to further improve the noise tolerance, we introduce an exponential normalization to smooth the complementary loss. Hence, the robust complementary loss for pair (I_i, T_i) could be formulated as:

$$\begin{aligned} \mathcal{L}_r(I_i, T_i, q) &= \mathcal{L}_r^\circ(I_i, T_i, q) + \mathcal{L}_r^\diamond(T_i, I_i, q) \\ &= \sum_{j \neq i}^N \tan(p_{ij}^\circ) / \left(\sum_{k=1}^N \tan(p_{ik}^\circ) \right)^q + \sum_{j \neq i}^N \tan(p_{ji}^\diamond) / \left(\sum_{k=1}^N \tan(p_{ki}^\diamond) \right)^q, \end{aligned} \quad (6)$$

where $\tan(\cdot)$ is the tan function and $q \in [0, 1]$ is a regulatory factor. Theoretically, for any input (I_i, T_i) under noise rate $\eta \leq \frac{N-1}{N}$, we can show (see proofs in supplementary material)

$$C \leq R_{\mathcal{L}_r}(f^*) - R_{\mathcal{L}_r}(f_\eta^*) \leq 0, \quad (7)$$

where $C = 2\eta(A_{\min}^{(1-q)} - A_{\max}^{(1-q)}) / (1 - \frac{N\eta}{N-1}) \leq 0$. C increases as q increases and when $q = 1$, C takes the maximum value 0. A_{\min} and A_{\max} are the maximum and minimum values of $\sum_{j=1}^N \tan(p_{ij})$ under the condition $\sum_{j=1}^N p_{ij} = 1$, where $1 < A_{\min} < A_{\max}$, and $0 \leq p_{ij} \leq 1$ ($p_{ij} = p_{ij}^\circ$ or p_{ij}^\diamond). f^* and f_η^* are the global minimizers of $R_{\mathcal{L}_r}(f)$ and $R_{\mathcal{L}_r}^\eta(f)$, respectively.

Analysis: The larger the q is, $C \rightarrow 0$, the tighter the bound of Equation (7) is. When $q = 0$, \mathcal{L}_r is a standard complementary contrastive loss [20]. In the extreme case of $q = 1$, $R_{\mathcal{L}_r}(f^*) = R_{\mathcal{L}_r}(f_\eta^*)$, *i.e.*, \mathcal{L}_r is noise tolerant since f_η^* and f^* are simultaneously the minimizers of $R_{\mathcal{L}_r}(f)$ (It can also be obtained from Lemma 1 that \mathcal{L}_r is robust under $q = 1$). Put another way, as q approaches 1, the optimum f_η^* of the noisy risk will be close to f^* on the clean data more likely, which implies noise tolerance.

Like most robust learning methods [32, 33], we should focus more on reliable data, while less on unreliable data. In other words, a smaller value of q is used for more convincing pairs (with larger \hat{y}_{ii}), while a larger value of q is for less convincing pairs (with smaller \hat{y}_{ii}). Thus, we could empirically utilize the soft corrected label \hat{y}_{ii} to recast q like the soft margin used in NCR [12], *i.e.*, $q = 1 - \hat{y}_{ii}$. However, indirect learning will face the underfitting problem, resulting in suboptimal/insufficient performance. To address this issue, we introduce a weighted active learning loss \mathcal{L}_d to make the model pay more attention to positive/matched pairs, *i.e.*, $\mathcal{L}_d(I_i, T_i, \hat{y}_{ii}) = -\hat{y}_{ii} (\log p_{ii}^\circ + \log p_{ii}^\diamond)$. This positive learning will mine discrimination from direct supervision, which complements the complementary learning loss. By combining active and complementary learning losses, our active complementary loss is defined as:

$$\mathcal{L}_{acl}(I_i, T_i, \hat{y}_{ii}) = \mathcal{L}_d(I_i, T_i, \hat{y}_{ii}) + \lambda \mathcal{L}_r(I_i, T_i, 1 - \hat{y}_{ii}), \quad (8)$$

where λ is a scale factor to prevent \mathcal{L}_d from dominating the cross-modal training and quickly overfitting NC. As shown in Equation (8), when (I_i, T_i) is a noisy pair and \hat{y}_{ii} ideally approaches 0, the loss emphasizes robust complementary learning, thus mitigating overfitting to NC. Conversely, when (I_i, T_i) is a clean pair and \hat{y}_{ii} ideally approaches 1, the loss focuses on discriminative learning, thereby facilitating the accurate acquisition of visual-semantic associations. However, due to computational resource constraints, we cannot use the entire training set to perform cross-modal learning. Therefore,

we relax N to the size K of the mini-batch \mathbf{x} by Monte Carlo sampling. Without loss of generality, the final loss for cross-modal learning is given by:

$$\mathcal{L}_{acl}(\mathbf{x}) = \frac{1}{K} \sum_{i=1}^K \mathcal{L}_{acl}(I_i, T_i, \hat{y}_{ii}). \quad (9)$$

Lemma 1. *In an instance-level cross-modal matching problem, under uniform NC with noise rate $\eta \leq \frac{N-1}{N}$, when $q = 1$, \mathcal{L}_r is noise tolerant.*

Proof. The proofs of Equation (7) and Lemma 1 can be found in the supplementary material. \square

2.3 Self-refining Correspondence Correction

Another key to solving NC is how to obtain accurate correspondence estimations so as to reduce the adverse effects of NC. To this end, we propose an effective Self-refining Correspondence Correction paradigm (SCC). SCC leverages Momentum Correction (MC) to aggregate historical predictions, providing stable and accurate correspondence estimations while alleviating the over-memorization to NC. To eliminate the error accumulation against NC, we combine multiple independent Self-Refining (SR) in the entire training process. Specifically, the MC for the correspondence of (I_i, T_i) at the t -th epoch is defined as follows:

$$y_{ii}^t = \beta y_{ii}^{t-1} + (1 - \beta) \hat{p}^t(I_i, T_i), \quad (10)$$

where $\beta \in (0, 1)$ represents the momentum coefficient, $\hat{p}^t(I_i, T_i) = (p_{ii}^o + p_{ii}^s)/2$ denotes the average matching probability at the t -th epoch. Through adequate cross-modal training, our CRCL will obtain a more stable and accurate soft correspondence label by smoothly evolving and expanding the receptive field of correction based on historical predictions with MC. Notably, as training progresses, some pairs would always be incorrectly distinguished as clean or noisy ones, resulting in the error accumulation of the estimated labels (see Figure 3c). Additionally, even though the updates performed by MC help reduce the negative influence of NC, the initial correspondence label (y_{ii}^0) still greatly affects the quality of subsequent smooth corrections. In other words, providing more accurate initial correspondences weakens the DNN’s memorization against NC, thereby reducing the risk of error accumulation.

Algorithm 1: The pseudo-code of CRCL

Input: A noisy training dataset \mathcal{D}_η , image-text matching model $\mathcal{M}(\Theta)$;

Initialize: Θ ;

for e^j in $[e_1, e_2, \dots, e_m]$ **do**

for t in $[1, 2, \dots, e^j]$ **do**

for \mathbf{x} in batches **do**

 Obtain the bidirectional matching probabilities of \mathbf{x} with Equation (3);

 Update the correspondence labels with Equation (11);

 Obtain the corrected labels with Equation (12);

 Compute the overall loss $\mathcal{L}_{acl}(\mathbf{x})$ with Equation (9);

$\Theta = \text{Optimizer}(\Theta, \mathcal{L}_{acl}(\mathbf{x}))$;

end

end

 Re-initialize Θ ;

end

Output: The learned parameters $\hat{\Theta}$;

To achieve accurate initial correspondence estimations, SCC refines updated correspondence labels historically in epochs using MC through multiple concatenated SR pieces during the entire training process. Subsequent SR pieces could gradually aggregate the learned correspondence knowledge from previous pieces, thus improving the quality of estimated correspondences progressively. Furthermore, each SR piece is trained from scratch, which aims to clear accumulated error/noise that has been memorized, thus providing more accurate correspondence predictions for subsequent training. Mathematically, SCC consists of multiple SR pieces $([e_1, \dots, e_m])$ based on MC, where each piece

undergoes robust learning for e_j ($j \in \{1, \dots, m\}$) epochs. Thus, during the j -th SR training, the estimated soft label of the i -th pair at t -th epoch is reconsidered as follows:

$$y_{ii}^{(j,t)} = \begin{cases} y_{ii}^{(j-1, e_{j-1})}, & \text{if } t \leq e_f, \\ \hat{p}^{(j, t-1)}(I_i, T_i), & \text{if } j = 1 \text{ and } t = (e_f + 1), \\ \beta y_{ii}^{(j, t-1)} + (1 - \beta) \hat{p}^{(j, t-1)}(I_i, T_i), & \text{otherwise,} \end{cases} \quad (11)$$

where $\hat{p}^{(j, t-1)}(*)$ is the average matching probability of pair (I_i, T_i) at the $(t-1)$ -th epoch during the j -th training piece, e_f denotes the number of epochs to freeze the correspondence label, preventing insufficient model training in the early stage from affecting the correction quality. In our experiments, we set all initial labels to 1, assuming that all training pairs are matched at the beginning of the first SR piece. In practice, we assign the label of the confident noisy pair as 0 to reduce the risk of producing erroneous supervision information. Therefore, the final corrected correspondence label used for \mathcal{L}_{acl} is defined as:

$$\hat{y}_{ii} = \begin{cases} 0, & \text{if } y_{ii}^{(j,t)} < \epsilon, \\ y_{ii}^{(j,t)}, & \text{otherwise,} \end{cases} \quad (12)$$

where $\epsilon = 0.1$ is a fixed threshold used to filter the confident noisy pairs in experiments.

3 Experiments

In this section, comprehensive experiments are conducted on three widely used benchmarks to demonstrate the robustness and effectiveness of our CRCL under multiple scenarios, including synthetic noise, real-world noise, and well-annotated correspondence.

3.1 Datasets and Protocols

Datasets: For an extensive evaluation, we use three benchmark datasets (*i.e.*, Flickr30K [34], MS-COCO [35] and CC152K [12]) in our experiments. More specifically, Flickr30K is a widely-used image-text dataset collected from the Flickr website, which comprises 31,000 images and each one has 5 corresponding textual descriptions. Following [36], 30,000 images are employed for training, 1,000 images for validation, and 1,000 images for testing in our experiments. MS-COCO is a large-scale image-text dataset, which has 123,287 images, and 5 captions are given to describe each image. We follow the split of [36, 8] to carry out our experiments, *i.e.*, 5000 validation images, 5000 test images, and the rest for training. CC152K is a subset of Conceptual Captions (CC) [10] collected in the real world, which is selected by [12]. Due to the absence of manual annotation, there are about 3% \sim 20% incorrect correspondences in CC, *i.e.*, real-world noisy correspondences. CC152K contains 150,000 image-text pairs for training, 1,000 pairs for validation, and 1,000 pairs for testing.

Evaluation Protocols: Recall at K (R@K=1, 5, and 10) is used to measure the performance of bidirectional retrievals, which is defined as the proportion of the queries with the correct item in the top K retrieved results. Besides, flowing [19], we also take the sum of all Recalls to evaluate the overall performance, *i.e.*, rSum.

3.2 Implementation Details

Our CRCL is a generalized robust framework that could extend existing methods to confront noisy correspondences. To demonstrate the effectiveness and robustness of CRCL, we extend two representative methods, *i.e.*, VSE $_{\infty}$ [9] and SGRAF (SGR and SAF) [4], to perform robust image-text matching, respectively. Specifically, the shared hyper-parameters are set as the same as the original works [4, 9], *e.g.*, the batch size is 128, the word embedding size is 300, and the joint embedding dimensionality is 1,024. More specific hyper-parameters and implementation details are given in our supplementary material due to the space limitation.

3.3 Comparison with State-of-the-Arts

In this section, we evaluate our CRCL by comparing it with 7 state-of-the-art methods on three benchmarks, *i.e.*, SCAN (ECCV'18) [8], SGRAF (SGR and SAF, AAAI'21) [4], VSE $_{\infty}$ (CVPR'21) [9], NCR (NeurIPS'21) [12], DECL (ACM MM'22) [19], BiCro (CVPR'23) [23] and MSCN

(CVPR’23) [24]. For a fair comparison, all tested approaches adopt the same visual features (BUTD features) [8] and textual backbone Bi-GRU [37]. To comprehensively investigate the robustness of our method, we artificially inject synthetic false correspondence of different ratios by proportionally shuffling the captions on Flickr30K and MS-COCO like [12], *i.e.*, 20%, 40%, 60%, and 80% noise rates. In addition to synthetic noise, we also evaluate the robustness of tested methods against the real-world noisy correspondences on CC152K. Due to the space limitation, we only provide the results on MS-COCO 5K under well-annotated correspondences in Table 2. For fairness, like [19, 23], the ensemble results of CRCL-SGRAF are reported in the paper. More extensive comparison results are provided in the supplementary material to fully demonstrate the superiority of CRCL.

Table 1: Performance comparison (R@K(%) and rSum) of image-text matching on Flickr30K and MS-COCO 1K. The highest scores are shown in **bold**. ‘*’ means robust methods.

Noise	Methods	Flickr30K							MS-COCO 1K						
		Image → Text			Text → Image			rSum	Image → Text			Text → Image			rSum
		R@1	R@5	R@10	R@1	R@5	R@10	rSum	R@1	R@5	R@10	R@1	R@5	R@10	rSum
20%	SCAN	56.4	81.7	89.3	34.2	65.1	75.6	402.3	28.9	64.5	79.5	20.6	55.6	73.5	322.6
	SAF	51.8	79.5	88.3	38.1	66.8	76.6	401.1	41.0	78.4	89.4	38.2	74.0	85.5	406.5
	SGR	61.2	84.3	91.5	44.5	72.1	80.2	433.8	49.1	83.8	92.7	42.5	77.7	88.2	434.0
	VSE ∞	69.0	89.2	94.8	48.8	76.3	83.8	461.9	73.5	93.3	97.0	57.4	86.5	92.8	500.5
	NCR*	76.7	93.9	96.9	57.5	82.8	89.2	497.0	77.0	95.6	98.1	61.5	89.3	95.1	516.6
	DECL*	75.6	93.8	97.4	58.5	82.9	89.4	497.6	77.1	95.9	98.4	61.6	89.1	95.2	517.3
	BiCro*	78.1	94.4	97.5	60.4	84.4	89.9	504.7	78.8	96.1	98.6	63.7	90.3	95.7	523.2
	MSCN*	77.4	94.9	97.6	59.6	83.2	89.2	501.9	78.1	97.2	98.8	64.3	90.4	95.8	524.6
CRCL*	77.9	95.4	98.3	60.9	84.7	90.6	507.8	79.6	96.1	98.7	64.7	90.6	95.9	525.6	
40%	SCAN	29.9	60.5	72.5	16.4	38.5	48.6	266.4	30.1	65.2	79.2	18.9	51.1	69.9	314.4
	SAF	34.3	65.6	78.4	30.1	58.0	68.5	334.9	36.0	74.4	87.0	33.7	69.4	82.5	383.0
	SGR	47.2	76.4	83.2	34.5	60.3	70.5	372.1	43.9	78.3	89.3	37.0	72.8	85.1	406.4
	VSE ∞	30.2	58.3	70.2	22.3	49.6	62.7	293.3	53.3	84.3	92.1	31.4	63.8	75.0	399.9
	NCR*	75.3	92.1	95.2	56.2	80.6	87.4	486.8	76.5	95.0	98.2	60.7	88.5	95.0	513.9
	DECL*	72.5	93.1	97.0	55.8	81.2	88.1	487.7	77.1	95.7	98.3	61.5	89.2	95.3	517.1
	BiCro*	74.6	92.7	96.2	55.5	81.1	87.4	487.5	77.0	95.9	98.3	61.8	89.2	94.9	517.1
	MSCN*	74.4	94.4	96.9	57.2	81.7	87.6	492.2	74.8	94.9	98.0	60.3	88.5	94.4	510.9
CRCL*	77.8	95.2	98.0	60.0	84.0	90.2	505.2	78.2	95.7	98.3	63.3	90.3	95.7	521.5	
60%	SCAN	16.9	39.3	53.9	2.8	7.4	11.4	131.7	27.8	59.8	74.8	16.8	47.8	66.4	293.4
	SAF	28.3	54.5	67.5	22.1	47.3	59.0	278.7	28.2	63.9	79.4	31.1	65.6	80.5	348.7
	SGR	28.7	58.0	71.0	23.8	49.5	60.7	291.7	37.6	73.3	86.3	33.8	68.6	81.7	381.3
	VSE ∞	18.0	44.0	55.7	15.1	38.5	51.8	223.1	33.4	64.8	79.1	26.0	60.1	76.3	339.7
	NCR*	68.7	89.9	95.5	52.0	77.6	84.9	468.6	72.7	94.0	97.6	57.9	87.0	94.1	503.3
	DECL*	69.4	89.4	95.2	52.6	78.8	85.9	471.3	73.8	94.7	97.7	59.6	87.9	94.5	508.2
	BiCro*	67.6	90.8	94.4	51.2	77.6	84.7	466.3	73.9	94.4	97.8	58.3	87.2	93.9	505.5
	MSCN*	70.4	91.0	94.9	53.4	77.8	84.1	471.6	74.4	95.1	97.9	59.2	87.1	92.8	506.5
CRCL*	73.1	93.4	95.8	54.8	81.9	88.3	487.3	76.3	95.1	97.9	60.8	89.0	95.1	514.2	
80%	SCAN	5.1	18.1	27.3	3.9	13.1	19.1	86.6	22.2	51.9	67.5	13.8	41.1	58.6	255.1
	SAF	12.2	32.8	48.4	11.8	30.5	41.5	177.2	24.2	57.5	74.1	24.7	57.1	73.0	310.6
	SGR	13.7	35.1	47.6	12.1	30.9	41.9	181.3	26.7	60.7	75.6	25.3	58.2	72.6	319.1
	VSE ∞	8.1	23.1	34.7	7.4	22.6	31.8	127.7	25.4	55.1	70.6	19.2	50.5	68.0	288.8
	NCR*	1.4	7.1	11.7	1.5	5.4	9.3	36.4	21.6	52.6	67.6	15.1	38.1	49.8	244.8
	DECL*	60.7	84.6	91.2	42.1	69.6	78.6	426.8	65.6	91.6	96.6	52.0	83.0	91.3	480.1
	BiCro*	3.6	13.9	20.5	1.7	7.5	13.0	60.2	40.0	72.6	84.7	22.6	53.0	67.2	340.1
	MSCN*	1.0	4.4	9.1	0.4	1.4	2.5	18.8	66.8	91.6	96.2	52.7	83.0	90.9	481.2
CRCL*	62.3	86.8	92.8	46.0	73.6	82.2	443.7	72.7	93.5	97.6	57.5	86.8	93.7	501.8	

3.3.1 Results under Synthetic Noisy Correspondences

For quantitative evaluation under specific noise levels, we conduct all tested methods under four different noise rates (*i.e.*, 20%, 40%, 60%, and 80%) of synthetic noisy correspondences on the Flickr30K and MS-COCO datasets. Quantitative results on Flickr30K and MSCOCO 1K test set are shown in Table 6. For MS-COCO, the results are computed by a veraging over 5 folds of 1K test images. From the results, one can see that our CRCL could remarkably outperform the robust baselines (NCR, DECL, BiCro, and MSCN) on most of the metrics, which demonstrates the superior robustness of CRCL against NC. Moreover, our CRCL not only performs well in low noise but also achieves the best performance under high noise, especially 80% noise, which provides strong evidence for the stability and robustness of our method.

Table 2: Performance comparison on CC152K and MS-COCO 5K.

Methods	CC152K							MS-COCO 5K						
	Image \rightarrow Text			Text \rightarrow Image				rSum	Image \rightarrow Text			Text \rightarrow Image		
	R@1	R@5	R@10	R@1	R@5	R@10			R@1	R@5	R@10	R@1	R@5	R@10
SCAN	30.5	55.3	65.3	26.9	53.0	64.7	295.7	44.7	75.9	86.6	33.3	63.5	75.4	379.4
VSE $_{\infty}$	34.0	64.5	77.0	12.9	19.2	21.6	229.2	56.6	83.6	91.4	39.3	69.9	81.1	421.9
SGRAF	32.5	59.5	70.0	32.5	60.7	68.7	323.9	58.8	84.8	92.1	41.6	70.9	81.5	429.7
NCR*	39.5	64.5	73.5	40.3	64.6	73.2	355.6	58.2	84.2	91.5	41.7	71.0	81.3	427.9
DECL*	39.0	66.1	75.5	40.7	66.3	76.7	364.3	59.2	84.5	91.5	41.7	70.6	81.1	428.6
MSCN*	40.1	65.7	76.6	40.6	67.4	76.3	366.7	-	-	-	-	-	-	-
BiCro*	40.8	67.2	76.1	42.1	67.6	76.4	370.2	59.0	84.4	91.7	42.4	71.2	81.7	430.4
CRCL*	41.8	67.4	76.5	41.6	68.0	78.4	373.7	61.3	85.8	92.7	43.5	72.6	82.7	438.6

3.3.2 Results under Real Noisy Correspondences

In addition to synthetic noise, we carry the comparison experiments on the real-world noisy dataset CC152K. The quantitative results are shown in Table 2. From the results, one can see that our CRCL is superior to all baselines with the best overall performance of 373.7%, which indicates that the proposed method is robust against real-world noise. Specifically, CRCL outperforms the best baseline BiCro, with absolute performance improvement of 1.0%, 0.2%, 0.4%, 0.4%, and 2.0% across different metrics, except for R@1 in text-to-image retrieval.

3.3.3 Results under Well-annotated Correspondences

Besides noisy correspondences, we also evaluate the tested methods trained on the well-aligned MS-COCO dataset for a comprehensive comparison. The results on MS-COCO 5K are shown in Table 2, wherein the results of all baselines are reported by the original papers for a fair comparison, except for the reproduced results of BiCro. From the table, our CRCL remarkably outperforms all baselines in terms of rSum. Specifically, CRCL prevails over the best baselines by 8.2% on overall performance (*i.e.*, rSum) absolutely, which shows that our CRCL is not only suitable for noisy cases but also performs well in well-aligned ones.

3.4 Comparison to pre-trained model

In this section, we compare our CRCL to the pre-trained model CLIP [38] to further evaluate its effectiveness in handling NC. CLIP is a well-known large pre-trained model that is trained from scratch on a dataset of 400 million image-text pairs collected from the Internet, which includes a large number of training pairs with real NCs. More specifically, following [12], we report the zero-shot results and fine-tuning results under 20% noise and compare them with that of CRCL-SGRAF in Table 3. From the results, CLIP shows a significant performance drop during fine-tuning under NC. On the contrary, the performance of our CRCL under 20% noise is even better than the zero-shot result of CLIP (ViT-L/14), which shows the strength and potential of our CRCL in dealing with NC.

Table 3: Comparison with CLIP on MS-COCO 5K.

Noise Rate	Methods	Image \rightarrow Text			Text \rightarrow Image			rSum
		R@1	R@5	R@10	R@1	R@5	R@10	
0%, Zero-Shot	CLIP (ViT-L/14)	58.4	81.5	88.1	37.8	62.4	72.2	400.4
	CLIP (ViT-B/32)	50.2	74.6	83.6	30.4	56.0	66.8	361.6
20%, Fine-tune	CLIP (ViT-L/14)	36.1	61.3	72.5	22.6	43.2	53.7	289.4
	CLIP (ViT-B/32)	21.4	49.6	63.3	14.8	37.6	49.6	236.3
	Our CRCL	59.3	85.2	91.9	42.9	71.9	82.1	433.3

3.5 Ablation Study

In this section, we present ablation studies conducted on Flickr30K with 60% noise, as shown in Table 4. From the table, one can find that the full version of our CRCL achieves the best performance, which indicates that each component contributes to our method for performance improvement. By recasting q with the rectified label \hat{y}_{ii} using SCC, \mathcal{L}_r shows higher potential against NC. Moreover,

through the combination of active learning and robust complementary learning, there is further performance improvement, which indicates the effectiveness of our ACL. Note that these results are obtained from a single model for a comprehensive evaluation, and are not ensemble results as shown in Tables 2 and 6.

Table 4: Ablation studies on Flickr30K with 60% noise.

Configuration	loss	SCC	Image \rightarrow Text			Text \rightarrow Image			rSum
			R@1	R@5	R@10	R@1	R@5	R@10	
\mathcal{L}_{acl}	✓		70.5	91.3	95.6	52.5	79.4	86.8	476.1
\mathcal{L}_d	✓		69.3	91.1	95.2	51.4	78.2	86.0	471.2
\mathcal{L}_r	✓		67.7	91.2	95.0	52.3	79.0	86.4	471.6
$\mathcal{L}_r(q=1)$			25.2	53.9	65.6	20.3	45.0	57.2	267.2
$\mathcal{L}_r(q=0)$			63.5	89.7	93.8	48.2	74.5	82.0	451.7
\mathcal{L}_d			65.6	87.5	93.2	47.7	74.6	82.7	451.3

3.6 Visualization Analysis

To further investigate the generalization and robustness of CRCL, we visually study the retrieval performance of our CRCL-VSE ∞ , CRCL-SAF, and CRCL-SGR on Flickr30K and MS-COCO with varying noise rates in Figure 3(a,d). From the figure, one can see that CRCL can enhance the robustness of the original methods and perform well even under high noise. In addition, we provide visualization to intuitively showcase the effectiveness of the proposed SCC. Specifically, we visualize the distributions of both cross-modal similarities and corrected correspondences for noisy training pairs using CRCL-SGR on Flickr30K with 60% NCs. For comparison, we also visualize the results without SCC, where we replace \hat{y}_{ii} with the prediction $\hat{p}^t(I_i, T_i)$ for the current iteration. The visualizations clearly indicate that SCC prevents the over-accumulation of errors in correspondence correction, thus verifying its effectiveness in mitigating the impact of NC.

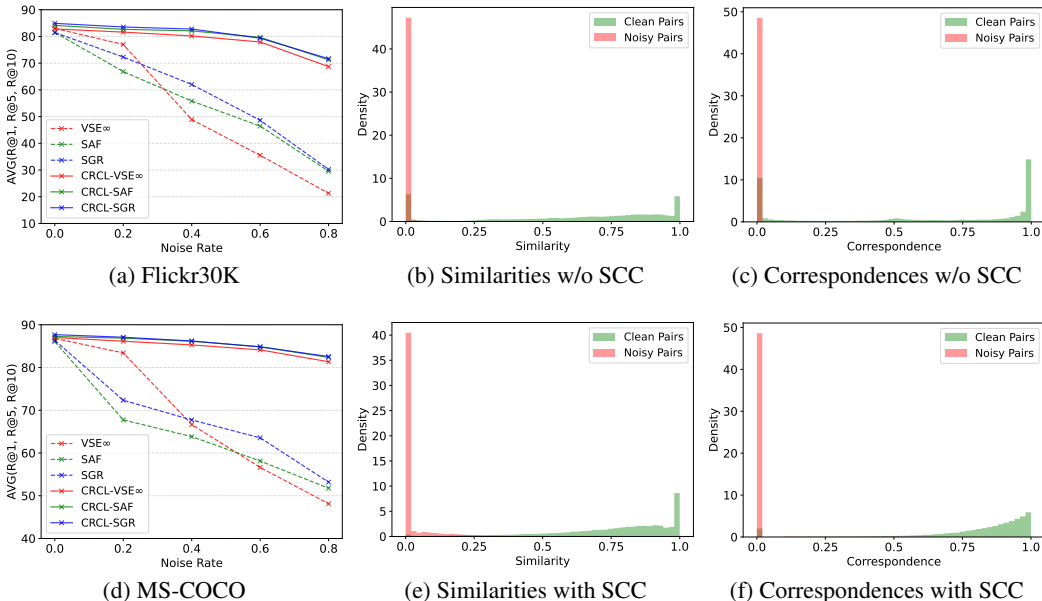


Figure 1: (a,d) The performance on Flickr30K and MS-COCO with varying noise rates; (b,c/e,f) The similarities and corrected correspondences of training pairs after learning without/with SCC.

4 Conclusion

In this paper, we propose a generalized robust framework CRCL to endow traditional methods with robustness against noisy correspondences. To alleviate the harmful effects brought by NC, we present

an Active Complementary Loss (ACL) and a Self-refining Correspondence Correction technique (SCC). These techniques enable effective learning of visual-semantic associations and progressive correction of correspondences based on historical predictions, thus boosting the robustness of image-text matching. Extensive experiments demonstrate that our CRCL achieves state-of-the-art robustness to both synthetic and real-world NCs. Furthermore, ablation studies and visualization analyses further verify the effectiveness and reliability of the proposed components.

5 Limitations and Broader Impact Statement

Despite the promising performance of our proposed CRCL, there are some limitations that should be acknowledged. First, we only study the NC problem between two modalities, *i.e.*, image and text. Second, we did not take into account category-level noise. The proposed CRCL likely impacts various applications that require robust image-text matching, *e.g.*, multimedia retrieval, and image annotation. We encourage further study to understand and mitigate the biases and risks potentially brought by image-text matching.

Acknowledgments and Disclosure of Funding

This work was supported by the National Natural Science Foundation of China (U19A2078, U21B2040, 62372315, 62176171, and 62102274), Sichuan Science and Technology Planning Project (2023YFQ0020, 2023YFG0033, 2023ZHCG0016, 2022YFQ0014, 2022YFH0021), Chengdu Science and Technology Project (2023-XT00-00004-GX), the SCU-LuZhou Sciences and Technology Cooperation Program (2023CDLZ-16), and Fundamental Research Funds for the Central Universities under Grant YJ202140.

References

- [1] Mateusz Malinowski, Marcus Rohrbach, and Mario Fritz. Ask your neurons: A neural-based approach to answering questions about images. In *Proceedings of the IEEE international conference on computer vision*, pages 1–9, 2015.
- [2] Oriol Vinyals, Alexander Toshev, Samy Bengio, and Dumitru Erhan. Show and tell: A neural image caption generator. In *Proceedings of the IEEE conference on computer vision and pattern recognition*, pages 3156–3164, 2015.
- [3] Kelvin Xu, Jimmy Ba, Ryan Kiros, Kyunghyun Cho, Aaron Courville, Ruslan Salakhudinov, Rich Zemel, and Yoshua Bengio. Show, attend and tell: Neural image caption generation with visual attention. In *International conference on machine learning*, pages 2048–2057. PMLR, 2015.
- [4] Haiwen Diao, Ying Zhang, Lin Ma, and Huchuan Lu. Similarity reasoning and filtration for image-text matching. In *Proceedings of the AAAI Conference on Artificial Intelligence*, volume 35, pages 1218–1226, 2021.
- [5] Ding Jiang and Mang Ye. Cross-modal implicit relation reasoning and aligning for text-to-image person retrieval. *arXiv preprint arXiv:2303.12501*, 2023.
- [6] Peng Hu, Hongyuan Zhu, Jie Lin, Dezhong Peng, Yin-Ping Zhao, and Xi Peng. Unsupervised contrastive cross-modal hashing. *IEEE Transactions on Pattern Analysis and Machine Intelligence*, pages 1–1, 2022.
- [7] Fartash Faghri, David J Fleet, Jamie Ryan Kiros, and Sanja Fidler. Vse++: Improving visual-semantic embeddings with hard negatives. *arXiv preprint arXiv:1707.05612*, 2017.
- [8] Kuang-Huei Lee, Xi Chen, Gang Hua, Houdong Hu, and Xiaodong He. Stacked cross attention for image-text matching. In *Proceedings of the European conference on computer vision (ECCV)*, pages 201–216, 2018.
- [9] Jiacheng Chen, Hexiang Hu, Hao Wu, Yuning Jiang, and Changhu Wang. Learning the best pooling strategy for visual semantic embedding. In *Proceedings of the IEEE/CVF conference on computer vision and pattern recognition*, pages 15789–15798, 2021.

- [10] Piyush Sharma, Nan Ding, Sebastian Goodman, and Radu Soricut. Conceptual captions: A cleaned, hypernymed, image alt-text dataset for automatic image captioning. In *Proceedings of the 56th Annual Meeting of the Association for Computational Linguistics (Volume 1: Long Papers)*, pages 2556–2565, 2018.
- [11] Chao Jia, Yinfei Yang, Ye Xia, Yi-Ting Chen, Zarana Parekh, Hieu Pham, Quoc Le, Yun-Hsuan Sung, Zhen Li, and Tom Duerig. Scaling up visual and vision-language representation learning with noisy text supervision. In *International Conference on Machine Learning*, pages 4904–4916. PMLR, 2021.
- [12] Zhenyu Huang, Guocheng Niu, Xiao Liu, Wenbiao Ding, Xinyan Xiao, Hua Wu, and Xi Peng. Learning with noisy correspondence for cross-modal matching. *Advances in Neural Information Processing Systems*, 34:29406–29419, 2021.
- [13] Mouxing Yang, Yunfan Li, Peng Hu, Jinfeng Bai, Jiancheng Lv, and Xi Peng. Robust multi-view clustering with incomplete information. *IEEE Transactions on Pattern Analysis and Machine Intelligence*, 45(1):1055–1069, 2022.
- [14] Mouxing Yang, Yunfan Li, Zhenyu Huang, Zitao Liu, Peng Hu, and Xi Peng. Partially view-aligned representation learning with noise-robust contrastive loss. In *Proceedings of the IEEE/CVF conference on computer vision and pattern recognition*, pages 1134–1143, 2021.
- [15] Jie Wen, Chengliang Liu, Shijie Deng, Yicheng Liu, Lunke Fei, Ke Yan, and Yong Xu. Deep double incomplete multi-view multi-label learning with incomplete labels and missing views. *IEEE Transactions on Neural Networks and Learning Systems*, 2023.
- [16] Xu Yang, Cheng Deng, Kun Wei, Junchi Yan, and Wei Liu. Adversarial learning for robust deep clustering. *Advances in Neural Information Processing Systems*, 33:9098–9108, 2020.
- [17] Huaiwen Zhang, Yang Yang, Fan Qi, Shengsheng Qian, and Changsheng Xu. Robust video-text retrieval via noisy pair calibration. *IEEE Transactions on Multimedia*, 2023.
- [18] Mouxing Yang, Zhenyu Huang, Peng Hu, Taihao Li, Jiancheng Lv, and Xi Peng. Learning with twin noisy labels for visible-infrared person re-identification. In *Proceedings of the IEEE/CVF Conference on Computer Vision and Pattern Recognition*, pages 14308–14317, 2022.
- [19] Yang Qin, Dezhong Peng, Xi Peng, Xu Wang, and Peng Hu. Deep evidential learning with noisy correspondence for cross-modal retrieval. In *Proceedings of the 30th ACM International Conference on Multimedia*, pages 4948–4956, 2022.
- [20] Peng Hu, Zhenyu Huang, Dezhong Peng, Xu Wang, and Xi Peng. Cross-modal retrieval with partially mismatched pairs. *IEEE Transactions on Pattern Analysis and Machine Intelligence*, pages 1–15, 2023.
- [21] Junnan Li, Richard Socher, and Steven CH Hoi. Dividemix: Learning with noisy labels as semi-supervised learning. *arXiv preprint arXiv:2002.07394*, 2020.
- [22] Bo Han, Quanming Yao, Xingrui Yu, Gang Niu, Miao Xu, Weihua Hu, Ivor Tsang, and Masashi Sugiyama. Co-teaching: Robust training of deep neural networks with extremely noisy labels. *Advances in neural information processing systems*, 31, 2018.
- [23] Shuo Yang, Zhaopan Xu, Kai Wang, Yang You, Hongxun Yao, Tongliang Liu, and Min Xu. Bicro: Noisy correspondence rectification for multi-modality data via bi-directional cross-modal similarity consistency. *arXiv preprint arXiv:2303.12419*, 2023.
- [24] Haochen Han, Kaiyao Miao, Qinghua Zheng, and Minnan Luo. Noisy correspondence learning with meta similarity correction. *arXiv preprint arXiv:2304.06275*, 2023.
- [25] Devansh Arpit, Stanisław Jastrzebski, Nicolas Ballas, David Krueger, Emmanuel Bengio, Maxinder S. Kanwal, Tegan Maharaj, Asja Fischer, Aaron Courville, Yoshua Bengio, and Simon Lacoste-Julien. A closer look at memorization in deep networks. In Doina Precup and Yee Whye Teh, editors, *Proceedings of the 34th International Conference on Machine Learning*, volume 70 of *Proceedings of Machine Learning Research*, pages 233–242. PMLR, 06–11 Aug 2017.
- [26] Aritra Ghosh, Himanshu Kumar, and P Shanti Sastry. Robust loss functions under label noise for deep neural networks. In *Proceedings of the AAAI conference on artificial intelligence*, volume 31, 2017.

- [27] Jianfeng Dong, Xirong Li, Chaoxi Xu, Shouling Ji, Yuan He, Gang Yang, and Xun Wang. Dual encoding for zero-example video retrieval. In *Proceedings of the IEEE/CVF conference on computer vision and pattern recognition*, pages 9346–9355, 2019.
- [28] Naresh Manwani and PS Sastry. Noise tolerance under risk minimization. *IEEE transactions on cybernetics*, 43(3):1146–1151, 2013.
- [29] Zhirong Wu, Yuanjun Xiong, Stella X Yu, and Dahua Lin. Unsupervised feature learning via non-parametric instance discrimination. In *Proceedings of the IEEE conference on computer vision and pattern recognition*, pages 3733–3742, 2018.
- [30] Mathilde Caron, Ishan Misra, Julien Mairal, Priya Goyal, Piotr Bojanowski, and Armand Joulin. Unsupervised learning of visual features by contrasting cluster assignments. *Advances in Neural Information Processing Systems*, 33:9912–9924, 2020.
- [31] Peng Hu, Xi Peng, Hongyuan Zhu, Liangli Zhen, and Jie Lin. Learning cross-modal retrieval with noisy labels. In *Proceedings of the IEEE/CVF Conference on Computer Vision and Pattern Recognition*, pages 5403–5413, 2021.
- [32] Xingjun Ma, Hanxun Huang, Yisen Wang, Simone Romano, Sarah Erfani, and James Bailey. Normalized loss functions for deep learning with noisy labels. In *International conference on machine learning*, pages 6543–6553. PMLR, 2020.
- [33] Zhilu Zhang and Mert Sabuncu. Generalized cross entropy loss for training deep neural networks with noisy labels. *Advances in neural information processing systems*, 31, 2018.
- [34] Peter Young, Alice Lai, Micah Hodosh, and Julia Hockenmaier. From image descriptions to visual denotations: New similarity metrics for semantic inference over event descriptions. *Transactions of the Association for Computational Linguistics*, 2:67–78, 2014.
- [35] Tsung-Yi Lin, Michael Maire, Serge Belongie, James Hays, Pietro Perona, Deva Ramanan, Piotr Dollár, and C Lawrence Zitnick. Microsoft coco: Common objects in context. In *European conference on computer vision*, pages 740–755. Springer, 2014.
- [36] Andrej Karpathy and Li Fei-Fei. Deep visual-semantic alignments for generating image descriptions. In *Proceedings of the IEEE conference on computer vision and pattern recognition*, pages 3128–3137, 2015.
- [37] Mike Schuster and Kuldip K Paliwal. Bidirectional recurrent neural networks. *IEEE transactions on Signal Processing*, 45(11):2673–2681, 1997.
- [38] Alec Radford, Jong Wook Kim, Chris Hallacy, Aditya Ramesh, Gabriel Goh, Sandhini Agarwal, Girish Sastry, Amanda Askell, Pamela Mishkin, Jack Clark, et al. Learning transferable visual models from natural language supervision. In *International conference on machine learning*, pages 8748–8763. PMLR, 2021.
- [39] Dimitri P Bertsekas. *Constrained optimization and Lagrange multiplier methods*. Academic press, 2014.
- [40] Peter Anderson, Xiaodong He, Chris Buehler, Damien Teney, Mark Johnson, Stephen Gould, and Lei Zhang. Bottom-up and top-down attention for image captioning and visual question answering. In *Proceedings of the IEEE conference on computer vision and pattern recognition*, pages 6077–6086, 2018.
- [41] Ryan Kiros, Ruslan Salakhutdinov, and Richard S Zemel. Unifying visual-semantic embeddings with multimodal neural language models. *arXiv preprint arXiv:1411.2539*, 2014.
- [42] Kunpeng Li, Yulun Zhang, Kai Li, Yuanyuan Li, and Yun Fu. Visual semantic reasoning for image-text matching. In *Proceedings of the IEEE/CVF international conference on computer vision*, pages 4654–4662, 2019.
- [43] Haoran Wang, Ying Zhang, Zhong Ji, Yanwei Pang, and Lin Ma. Consensus-aware visual-semantic embedding for image-text matching. In *Computer Vision—ECCV 2020: 16th European Conference, Glasgow, UK, August 23–28, 2020, Proceedings, Part XXIV 16*, pages 18–34. Springer, 2020.
- [44] Zheng Li, Caili Guo, Zerun Feng, Jenq-Neng Hwang, and Xijun Xue. Multi-view visual semantic embedding. *IJCAI*, 2022.
- [45] Zihao Wang, Xihui Liu, Hongsheng Li, Lu Sheng, Junjie Yan, Xiaogang Wang, and Jing Shao. Camp: Cross-modal adaptive message passing for text-image retrieval. In *Proceedings of the IEEE/CVF international conference on computer vision*, pages 5764–5773, 2019.

- [46] Hui Chen, Guiguang Ding, Xudong Liu, Zijia Lin, Ji Liu, and Jungong Han. Imram: Iterative matching with recurrent attention memory for cross-modal image-text retrieval. In *Proceedings of the IEEE/CVF conference on computer vision and pattern recognition*, pages 12655–12663, 2020.
- [47] Chunxiao Liu, Zhendong Mao, Tianzhu Zhang, Hongtao Xie, Bin Wang, and Yongdong Zhang. Graph structured network for image-text matching. In *Proceedings of the IEEE/CVF conference on computer vision and pattern recognition*, pages 10921–10930, 2020.
- [48] Yuhao Cheng, Xiaoguang Zhu, Jiuchao Qian, Fei Wen, and Peilin Liu. Cross-modal graph matching network for image-text retrieval. *ACM Transactions on Multimedia Computing, Communications, and Applications (TOMM)*, 18(4):1–23, 2022.
- [49] Kunpeng Li, Yulun Zhang, Kai Li, Yuanyuan Li, and Yun Fu. Image-text embedding learning via visual and textual semantic reasoning. *IEEE Transactions on Pattern Analysis and Machine Intelligence*, 2022.
- [50] Huatian Zhang, Zhendong Mao, Kun Zhang, and Yongdong Zhang. Show your faith: Cross-modal confidence-aware network for image-text matching. 2022.
- [51] Kun Zhang, Zhendong Mao, Quan Wang, and Yongdong Zhang. Negative-aware attention framework for image-text matching. In *Proceedings of the IEEE/CVF Conference on Computer Vision and Pattern Recognition*, pages 15661–15670, 2022.
- [52] Yuxiao Chen, Jianbo Yuan, Long Zhao, Tianlang Chen, Rui Luo, Larry Davis, and Dimitris N Metaxas. More than just attention: Improving cross-modal attentions with contrastive constraints for image-text matching. In *Proceedings of the IEEE/CVF Winter Conference on Applications of Computer Vision*, pages 4432–4440, 2023.
- [53] Yang Liu, Hong Liu, Huaqiu Wang, and Mengyuan Liu. Regularizing visual semantic embedding with contrastive learning for image-text matching. *IEEE Signal Processing Letters*, 29:1332–1336, 2022.
- [54] Yan Huang, Yuming Wang, Yunan Zeng, and Liang Wang. Mack: multimodal aligned conceptual knowledge for unpaired image-text matching. *Advances in Neural Information Processing Systems*, 35:7892–7904, 2022.
- [55] Shashank Goel, Hritik Bansal, Sumit Bhatia, Ryan Rossi, Vishwa Vinay, and Aditya Grover. Cyclip: Cyclic contrastive language-image pretraining. *Advances in Neural Information Processing Systems*, 35:6704–6719, 2022.
- [56] Zhengxin Pan, Fangyu Wu, and Bailing Zhang. Fine-grained image-text matching by cross-modal hard aligning network. In *Proceedings of the IEEE/CVF Conference on Computer Vision and Pattern Recognition*, pages 19275–19284, 2023.
- [57] Zheren Fu, Zhendong Mao, Yan Song, and Yongdong Zhang. Learning semantic relationship among instances for image-text matching. In *Proceedings of the IEEE/CVF Conference on Computer Vision and Pattern Recognition*, pages 15159–15168, 2023.
- [58] Yalan Qin, Chuan Qin, Xinpeng Zhang, Donglian Qi, and Guorui Feng. Nim-nets: Noise-aware incomplete multi-view learning networks. *IEEE Transactions on Image Processing*, 32:175–189, 2022.
- [59] Yanglin Feng, Hongyuan Zhu, Dezhong Peng, Xi Peng, and Peng Hu. Rono: Robust discriminative learning with noisy labels for 2d-3d cross-modal retrieval. In *Proceedings of the IEEE/CVF Conference on Computer Vision and Pattern Recognition (CVPR)*, pages 11610–11619, June 2023.
- [60] Yijie Lin, Mouxing Yang, Jun Yu, Peng Hu, Changqing Zhang, and Xi Peng. Graph matching with bi-level noisy correspondence. In *Proceedings of the IEEE/CVF international conference on computer vision*, 2023.
- [61] Yalan Qin, Xinpeng Zhang, Liquan Shen, and Guorui Feng. Maximum block energy guided robust subspace clustering. *IEEE Transactions on Pattern Analysis and Machine Intelligence*, 45(2):2652–2659, 2022.
- [62] Yalan Qin, Hanzhou Wu, Xinpeng Zhang, and Guorui Feng. Semi-supervised structured subspace learning for multi-view clustering. *IEEE Transactions on Image Processing*, 31:1–14, 2021.

- [63] Yilun Xu, Peng Cao, Yuqing Kong, and Yizhou Wang. L_dmi: A novel information-theoretic loss function for training deep nets robust to label noise. *Advances in neural information processing systems*, 32, 2019.
- [64] Yisen Wang, Xingjun Ma, Zaiyi Chen, Yuan Luo, Jinfeng Yi, and James Bailey. Symmetric cross entropy for robust learning with noisy labels. In *Proceedings of the IEEE/CVF International Conference on Computer Vision*, pages 322–330, 2019.
- [65] Yangdi Lu, Yang Bo, and Wenbo He. An ensemble model for combating label noise. In *Proceedings of the Fifteenth ACM International Conference on Web Search and Data Mining*, pages 608–617, 2022.
- [66] Giorgio Patrini, Alessandro Rozza, Aditya Krishna Menon, Richard Nock, and Lizhen Qu. Making deep neural networks robust to label noise: A loss correction approach. In *Proceedings of the IEEE conference on computer vision and pattern recognition*, pages 1944–1952, 2017.
- [67] Daiki Tanaka, Daiki Ikami, Toshihiko Yamasaki, and Kiyoharu Aizawa. Joint optimization framework for learning with noisy labels. In *Proceedings of the IEEE conference on computer vision and pattern recognition*, pages 5552–5560, 2018.
- [68] Yangdi Lu and Wenbo He. Selc: Self-ensemble label correction improves learning with noisy labels. In Lud De Raedt, editor, *Proceedings of the Thirty-First International Joint Conference on Artificial Intelligence, IJCAI-22*, pages 3278–3284. International Joint Conferences on Artificial Intelligence Organization, 7 2022. Main Track.

Supplementary Material

In this supplementary material, we provide additional information for CRCL. Specifically, we first give detailed proofs of Equation (13) and Lemma 2 in Appendix A. To improve the reproducibility of CRCL, in Appendix B, we provide comprehensive implementation details of our CRCL for different extended baselines (*i.e.*, VSE ∞ [9], SAF[4], and SGR[4]) on three datasets. In addition, we present richer additional experimental results and analysis in Appendix C, including parameter analysis, progressive analysis, and extra comparison results, to fully verify the effectiveness and superiority of CRCL. Finally, we supplemented related work in Appendix D to further discuss the related research background.

A Detailed Proofs

A.1 Proof for Equation (13)

$$C \leq R_{\mathcal{L}_r}(f^*) - R_{\mathcal{L}_r}(f_\eta^*) \leq 0, \quad (13)$$

where $C = 2\eta(A_{\min}^{(1-q)} - A_{\max}^{(1-q)})/(1 - \frac{N\eta}{N-1}) \leq 0$. C increases as q increases and when $q = 1$, C takes the maximum value 0. A_{\min} and A_{\max} are the maximum and minimum values of $\sum_{j=1}^N \tan(p_{ij})$ under the condition $\sum_{j=1}^N p_{ij} = 1$, where $1 < A_{\min} < A_{\max}$, and $0 \leq p_{ij} \leq 1$ ($p_{ij} = p_{ij}^\circ$ or p_{ij}^\diamond). f^* and f_η^* are the global minimizers of $R_{\mathcal{L}_r}(f)$ and $R_{\mathcal{L}_r}^\eta(f)$, respectively.

Proof. Recall that for any f ,

$$\begin{aligned} R_{\mathcal{L}_r}(f) &= R_{\mathcal{L}_r^\circ}(f) + R_{\mathcal{L}_r^\diamond}(f) \\ &= \mathbb{E}_{(I_i, T_i) \sim \mathcal{D}} [y_i \mathcal{L}_r^\circ(I_i, T_i, q)] + \mathbb{E}_{(I_i, T_i) \sim \mathcal{D}} [y_i \mathcal{L}_r^\diamond(T_i, I_i, q)] \\ &= \mathbb{E}_{(I_i, T_i) \sim \mathcal{D}} [\mathcal{L}_r^\circ(I_i, T_i, q)] + \mathbb{E}_{(I_i, T_i) \sim \mathcal{D}} [\mathcal{L}_r^\diamond(T_i, I_i, q)] \end{aligned}$$

For uniform noisy correspondence with noise rate η , we consider the image-to-text direction and have

$$\begin{aligned}
R_{\mathcal{L}_r^\circ}^\eta(f) &= \mathbb{E}_{(I_i, T_i) \sim \mathcal{D}_\eta} [\tilde{y}_i \cdot \mathcal{L}_r^\circ(I_i, T_i, q)] \\
&= \mathbb{E}_{(I_i, T_i) \sim \mathcal{D}} \left[(1 - \eta) \mathcal{L}_r^\circ(I_i, T_i, q) + \frac{\eta}{N-1} \sum_{j \neq i} \mathcal{L}_r^\circ(I_i, T_j, q) \right] \\
&= \mathbb{E}_{(I_i, T_i) \sim \mathcal{D}} \left[(1 - \eta) \mathcal{L}_r^\circ(I_i, T_i, q) + \frac{\eta}{N-1} \left((N-1) \Delta^{(1-q)} - \mathcal{L}_r^\circ(I_i, T_i, q) \right) \right] \\
&= \mathbb{E}_{(I_i, T_i) \sim \mathcal{D}} \left[\left(1 - \frac{N\eta}{N-1} \right) \mathcal{L}_r^\circ(I_i, T_i, q) + \eta \Delta^{(1-q)} \right],
\end{aligned}$$

where $\Delta = \sum_{j=1}^N \tan(p_{ij}^\circ) > 1$. Since Δ has the maximum and minimum values (A_{\min} and A_{\max} , we provide a solution in **Remark.**) under the condition $\sum_{j=1}^N p_{ij}^\circ = 1, 0 \leq p_{ij}^\circ \leq 1$, for any p_{ij}° , we have

$$\left(1 - \frac{N\eta}{N-1} \right) R_{\mathcal{L}_r^\circ}(f) + \eta A_{\min}^{(1-q)} \leq R_{\mathcal{L}_r^\circ}^\eta(f) \leq \left(1 - \frac{N\eta}{N-1} \right) R_{\mathcal{L}_r^\circ}(f) + \eta A_{\max}^{(1-q)}.$$

Similarly, the above equation also holds for $R_{\mathcal{L}_r^\circ}(f)$ and $R_{\mathcal{L}_r^\circ}^\eta(f)$, *i.e.*,

$$\left(1 - \frac{N\eta}{N-1} \right) R_{\mathcal{L}_r^\circ}(f) + \eta A_{\min}^{(1-q)} \leq R_{\mathcal{L}_r^\circ}^\eta(f) \leq \left(1 - \frac{N\eta}{N-1} \right) R_{\mathcal{L}_r^\circ}(f) + \eta A_{\max}^{(1-q)}.$$

Thus, for $R_{\mathcal{L}_r}^\eta(f)$ and $R_{\mathcal{L}_r}(f)$, under $\eta \leq \frac{N-1}{N}$, we have

$$\left(1 - \frac{N\eta}{N-1} \right) R_{\mathcal{L}_r}(f) + 2\eta A_{\min}^{(1-q)} \leq R_{\mathcal{L}_r}^\eta(f) \leq \left(1 - \frac{N\eta}{N-1} \right) R_{\mathcal{L}_r}(f) + 2\eta A_{\max}^{(1-q)}.$$

or equivalently,

$$(R_{\mathcal{L}_r}^\eta(f) - 2\eta A_{\max}^{(1-q)}) / \left(1 - \frac{N\eta}{N-1} \right) \leq R_{\mathcal{L}_r}(f) \leq (R_{\mathcal{L}_r}^\eta(f) - 2\eta A_{\min}^{(1-q)}) / \left(1 - \frac{N\eta}{N-1} \right).$$

Thus, for f_η^* ,

$$R_{\mathcal{L}_r}(f^*) - R_{\mathcal{L}_r}(f_\eta^*) \geq (R_{\mathcal{L}_r}^\eta(f^*) - R_{\mathcal{L}_r}^\eta(f_\eta^*)) / \left(1 - \frac{N\eta}{N-1} \right) + C \geq C, \quad (14)$$

or equivalently,

$$R_{\mathcal{L}_r}^\eta(f^*) - R_{\mathcal{L}_r}^\eta(f_\eta^*) \leq \left(1 - \frac{N\eta}{N-1} \right) (R_{\mathcal{L}_r}(f^*) - R_{\mathcal{L}_r}(f_\eta^*)) + C' \leq C', \quad (15)$$

where $C = 2\eta(A_{\min}^{(1-q)} - A_{\max}^{(1-q)}) / \left(1 - \frac{N\eta}{N-1} \right) \leq 0$, $C' = 2\eta(A_{\max}^{(1-q)} - A_{\min}^{(1-q)}) \geq 0$, f^* is a minimizer of $R_{\mathcal{L}_r}(f)$. Since f_η^* and f^* are the minimizers of $R_{\mathcal{L}_r}^\eta(f)$ and $R_{\mathcal{L}_r}(f)$, respectively, we have $R_{\mathcal{L}_r}^\eta(f^*) - R_{\mathcal{L}_r}^\eta(f_\eta^*) \geq 0$ or $R_{\mathcal{L}_r}(f^*) - R_{\mathcal{L}_r}(f_\eta^*) \leq 0$. Besides, it can be seen from Figure 2 that C/C' increases/decreases as q increases. In other words, under $\eta \leq \frac{N-1}{N}$, the larger q is, the tighter the bound of Equation (15)/Equation (14) is. When q is 1, then $R_{\mathcal{L}_r}(f^*) = R_{\mathcal{L}_r}(f_\eta^*)$ or $R_{\mathcal{L}_r}^\eta(f^*) = R_{\mathcal{L}_r}^\eta(f_\eta^*)$. This completes the proof.

Remark For the maximum value of $\sum_{j=1}^N \tan(p_{ij})$, For brevity, let $y = \sum_{j=1}^N \tan(p_{ij}) = \sum_{j=1}^N \tan(x_j)$ under the condition $\sum_{j=1}^N x_j = 1$ and $0 \leq x_j \leq 1$. For any $x_i, x_j \in [0, 1]$, we have

$$\tan(x_i + x_j) = \frac{\tan(x_i) + \tan(x_j)}{1 - \tan(x_i) \tan(x_j)}.$$

Since $0 \leq 1 - \tan(x_i) \tan(x_j) \leq 1$, we have

$$\tan(x_i + x_j) \geq (1 - \tan(x_i) \tan(x_j)) \tan(x_i + x_j) = \tan(x_i) + \tan(x_j).$$

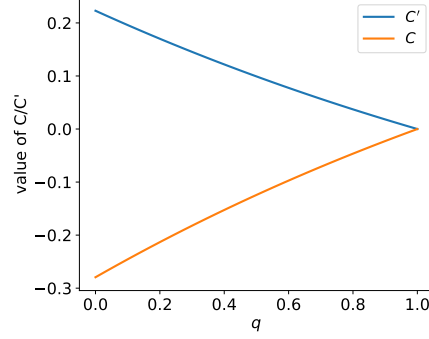


Figure 2: The value of C/C' changes with q , wherein N is 100 and η is 0.2.

Hence, $\sum_{j=1}^N \tan(x_j) \leq \tan(\sum_{j=1}^N x_j) = \tan 1$, i.e., $A_{max} = y_{max} = \tan 1 \approx 1.5574$.

For the minimum value of $y = \sum_{j=1}^N \tan(x_j)$, when $x_j \in (0, 1)$, $\frac{\partial y}{\partial x_j} = \frac{1}{\cos^2 x_j} > 0$. Thus, the minimum value does not appear on the hyperplane boundary (0 or 1). We use the Lagrange Multiplier method [39] to construct the objective as follows

$$\min y, \text{ s.t. } \sum_{j=1}^N x_j = 1 \Leftrightarrow \min_{x_j, \lambda} (y - \lambda(\sum_{j=1}^N x_j - 1)).$$

Let $f(x, \lambda) = y - \lambda(\sum_{j=1}^N x_j - 1) = \sum_{j=1}^N \tan(x_j) - \lambda(\sum_{j=1}^N x_j - 1)$, for x_j, λ , we have

$$\begin{cases} \frac{\partial f}{\partial x_j} = \frac{1}{\cos^2 x_j} - \lambda, & j = 1, 2, \dots, N, \\ \frac{\partial f}{\partial \lambda} = \sum_{j=1}^N x_j - 1. \end{cases}$$

Let $\frac{\partial f}{\partial x_j} = \frac{\partial f}{\partial \lambda} = 0$, we have

$$\begin{cases} \lambda = \frac{1}{\cos^2 x_j}, & j = 1, 2, \dots, N, \\ \sum_{j=1}^N x_j = 1. \end{cases}$$

Thus, when $x_1 = x_2 = \dots = x_N = \frac{1}{N}$, y has a minimum value, i.e., $A_{min} = y_{min} = N \tan \frac{1}{N} > 1$. \square

A.2 Proof for Lemma 2

Lemma 2. *In an instance-level cross-modal matching problem, under uniform NC with noise rate $\eta \leq \frac{N-1}{N}$, when $q = 1$, \mathcal{L}_r is noise tolerant.*

Proof. Recall that for any f ,

$$\begin{aligned} R_{\mathcal{L}_r}(f) &= R_{\mathcal{L}_r^\circ}(f) + R_{\mathcal{L}_r^\circ}(f) \\ &= \mathbb{E}_{(I_i, T_i) \sim \mathcal{D}} [y_i \mathcal{L}_r^\circ(I_i, T_i, q)] + \mathbb{E}_{(I_i, T_i) \sim \mathcal{D}} [y_i \mathcal{L}_r^\circ(T_i, I_i, q)] \\ &= \mathbb{E}_{(I_i, T_i) \sim \mathcal{D}} [\mathcal{L}_r^\circ(I_i, T_i, q)] + \mathbb{E}_{(I_i, T_i) \sim \mathcal{D}} [\mathcal{L}_r^\circ(T_i, I_i, q)] \end{aligned}$$

Under uniform noisy correspondence with noise rate η and $q = 1$, for any f , $R_{\mathcal{L}_r^\circ}^\eta(f)$ is written as

$$\begin{aligned}
R_{\mathcal{L}_r^\circ}^\eta(f) &= \mathbb{E}_{(I_i, T_i) \sim \mathcal{D}_\eta} [\tilde{y}_i \cdot \mathcal{L}_r^\circ(I_i, T_i, q = 1)] \\
&= \mathbb{E}_{(I_i, T_i) \sim \mathcal{D}} \left[(1 - \eta) \mathcal{L}_r^\circ(I_i, T_i, q = 1) + \frac{\eta}{N-1} \sum_{j \neq i} \mathcal{L}_r^\circ(I_i, T_j, q = 1) \right] \\
&= \mathbb{E}_{(I_i, T_i) \sim \mathcal{D}} \left[(1 - \eta) \mathcal{L}_r^\circ(I_i, T_i, q = 1) + \frac{\eta}{N-1} \left((N-2) + \frac{\tan(p_{ii}^\circ)}{\sum_{k=1}^N \tan(p_{ik}^\circ)} \right) \right] - \\
&= \mathbb{E}_{(I_i, T_i) \sim \mathcal{D}} \left[(1 - \eta) \mathcal{L}_r^\circ(I_i, T_i, q = 1) + \frac{\eta}{N-1} ((N-1) - \mathcal{L}_r^\circ(I_i, T_i, q = 1)) \right] \\
&= \left(1 - \frac{N\eta}{N-1}\right) R_{\mathcal{L}_r^\circ}(f) + \eta
\end{aligned} \tag{16}$$

Note that the equation between $R_{\mathcal{L}_r^\circ}^\eta(f)$ and $R_{\mathcal{L}_r^\circ}(f)$ can also be derived similarly as Equation (16), *i.e.*, $R_{\mathcal{L}_r^\circ}^\eta = \left(1 - \frac{N\eta}{N-1}\right) R_{\mathcal{L}_r^\circ}(f) + \eta$. Thus,

$$R_{\mathcal{L}_r}^\eta(f) = \left(1 - \frac{N\eta}{N-1}\right) R_{\mathcal{L}_r}(f) + 2\eta$$

Now, for any f , $R_{\mathcal{L}_r}^\eta(f^*) - R_{\mathcal{L}_r}^\eta(f) = \left(1 - \frac{N\eta}{N-1}\right) (R_{\mathcal{L}_r}(f^*) - R_{\mathcal{L}_r}(f)) \leq 0$, where $\eta \leq \frac{N-1}{N}$ and f^* is a global minimizer of $R_{\mathcal{L}_r}(f)$. This proves f^* is also the global minimizer of $R_{\mathcal{L}_r}^\eta(f)$. \square

B Implementation Details

B.1 Model Settings

In this section, we mainly detail the model settings and the implementation of CRCL. To comprehensively verify the effectiveness of our framework, we apply our CRCL to VSE $_\infty$ [9], SAF [4], and SGR [4] for further robustness against NC, *i.e.*, CRCL-VSE $_\infty$, CRCL-SAF, and CRCL-SGR. For the VSE model used in our CRCL-VSE $_\infty$, we use the same encoder models as VSE $_\infty$ [9] to project the local region features and word embeddings into the shared common space and then utilize GPO [9] to aggregate local representations into global representations, wherein the dimensionality of the common space is 1024. For the CRCL-SAF/SGR, like DECL [19], we directly perform our CRCL on the similarity output of these models without any changes to their models. In all experiments, we use the same image region features and text backbone for fairness. More specifically, we utilize a Faster R-CNN detection model [40] to extract local-level BUTD features of salient regions with top-36 confidence scores for each image, like [8, 4]. These features are encoded into a 2,048-dimensional feature vector and then projected into 1,024-dimensional image representations in the common space. For each text, the Bi-GRU language backbone encodes the word tokens into the same dimensional semantic vector space as the image representation. Following [9], we employ the size augmentation on the training data, which is then fed into the model. For all parameter settings, see Appendix B.2. The code of our CRCL will be released on GitHub.

B.2 Parameter Settings

In this section, we fully provide the parameter settings of our experiments in Table 5 for easy reproducibility on three benchmark datasets, *i.e.*, Flickr30K, MS-COCO, and CC152K. We divide the parameter settings into two groups, the first group includes the parameter settings for the training without synthetic noise ($=0\%$). The second group consists of the parameter settings for the training under synthetic noise ($> 0\%$). Simultaneously, each group details the training parameters of the three extensions of the baselines, *i.e.*, CRCL-VSE $_\infty$, CRCL-SAF, and CRCL-SGR. Note that the result of CRCL-SGRAF in the paper is the ensemble results of CRCL-SAF and CRCL-SGR. Following [4, 19, 23], the ensemble strategy is averaging the similarities computed by the two models and then performing image-text matching. Next, we will describe these main parameters. e_f represents the number of epochs to freeze the correspondence label, avoiding insufficient model training in the early stage from affecting the correction quality. e_i in $[e_1, \dots, e_m]$ is the number of training epochs for the i -th SR piece. During the last SR piece, CRCL decays the learning rate (lr_rate) by 0.1 in lr_update

epochs. τ and λ are the temperature parameter and the scale factor in ACL loss, respectively. β and ϵ are the momentum coefficient and the similarity threshold in SCC, respectively. For the parametric analysis of some hyper-parameters, see Appendix C.2 for more details.

Table 5: The settings of some key parameters for training on three datasets.

Noise	Datasets	Methods	e_f	$[e_1, \dots, e_m]$	lr_update	lr_rate	β	τ	λ	ϵ
Synthetic noise = 0%	CC152K	CRCL-VSE $_{\infty}$	2	[7,7,7,32]	17	0.0005	0.8	0.05	5	0.1
		CRCL-SAF	2	[7,7,7,42]	20	0.0005	0.8	0.05	5	0.1
		CRCL-SGR	2	[7,7,7,42]	20	0.0005	0.8	0.05	5	0.1
	Flickr30K	CRCL-VSE $_{\infty}$	2	[7,7,7,32]	15	0.0005	0.8	0.05	5	0.1
		CRCL-SAF	2	[7,7,7,32]	15	0.0005	0.8	0.05	5	0.1
		CRCL-SGR	2	[7,7,7,32]	15	0.0005	0.8	0.05	5	0.1
	MS-COCO	CRCL-VSE $_{\infty}$	2	[4,4,4,22]	12	0.0005	0.8	0.05	5	0.1
		CRCL-SAF	2	[4,4,4,22]	12	0.0005	0.8	0.05	5	0.1
		CRCL-SGR	2	[4,4,4,22]	12	0.0005	0.8	0.05	5	0.1
Synthetic noise > 0%	Flickr30K	CRCL-VSE $_{\infty}$	2	[7,7,7,32]	15	0.0005	0.8	0.05	5	0.1
		CRCL-SAF	2	[7,7,7,32]	15	0.0005	0.8	0.05	5	0.1
		CRCL-SGR	2	[7,7,7,32]	15	0.0005	0.8	0.05	5	0.1
	MS-COCO	CRCL-VSE $_{\infty}$	2	[4,4,4,22]	12	0.0005	0.8	0.05	5	0.1
		CRCL-SAF	2	[4,4,4,22]	12	0.0005	0.8	0.05	5	0.1
		CRCL-SGR	2	[4,4,4,22]	12	0.0005	0.8	0.05	5	0.1

C Additional Experiments and Analysis

C.1 Parametric Analysis

The proposed CRCL has three sensitive key hyper-parameters, *i.e.*, the temperature parameter τ , the momentum coefficient β , and the similarity threshold ϵ . Thus, we conduct detailed parameter experiments (shown in Figure 3) on the Flickr30K dataset to evaluate the impact of different hyper-parameter settings and obtain better parameter settings for CRCL. Note that all parametric experiments are performed by CRCL-VSE $_{\infty}$ under 60% noise. As can be seen from Figure 3a, too large or too small τ both cause a performance drop. Thus, in all experiments, we recommend the range of τ is 0.03 ~ 0.07. From Figure 3b, when the value of β is set to two extreme values, *i.e.*, 0 and 1, the performance drops remarkably. Moreover, in the range of (0, 1), as β increases, the performance gradually improves. We think that with the increase of β , each correction performed by MC will retain more historical information to reduce perturbation. Thus providing more stable corrected correspondences for training. In all our experiments, β is 0.8. From Figure 3c, we can see that proper filtering is beneficial for mitigating NC. We think this filtering strategy can prevent the active loss from exploiting these confident noisy pairs to produce more misleading gradients. Thus, we set ϵ as 0.1 in all our experiments.

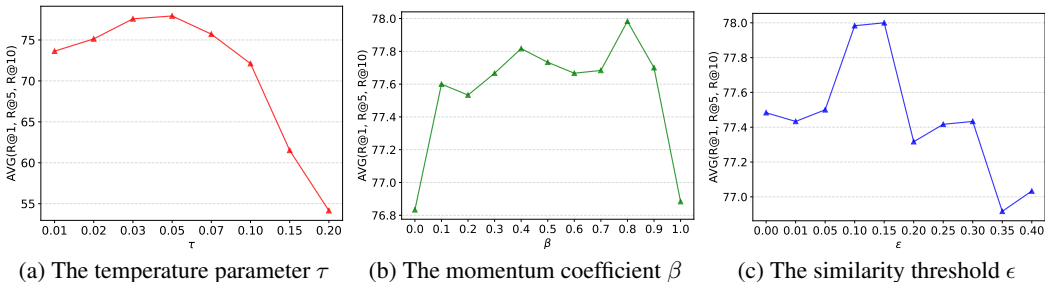


Figure 3: Parametric analysis on Flickr30K with 60% noise.

C.2 Progressive Analysis

To comprehensively investigate the effectiveness of our CRCL, we carry out some progressive processes to further analyze the advantages of CRCL. Specifically, we recorded the performance

of VSE_∞ with different loss functions, including CRCL- VSE_∞ , \mathcal{L}_d , $\mathcal{L}_r(q=1)$, $\mathcal{L}_r(q=0)$, Complementary Contrastive Loss (CCL) [20], the hinge-based Triplet Ranking loss (TR) [41], the Triplet Ranking loss with Hard Negatives (TR-HN) [7], on Flickr30K under 80% noise. We visualize the performance of bidirectional retrieval in Figure 4. From the results, although $\mathcal{L}_r(q=1)$ is noise-tolerant, which is consistent with the theoretical analysis (lemma 2), there would be some underfitting. Our CRCL with ACL loss fully explores the advantages of \mathcal{L}_r and \mathcal{L}_q , showing remarkable robustness.

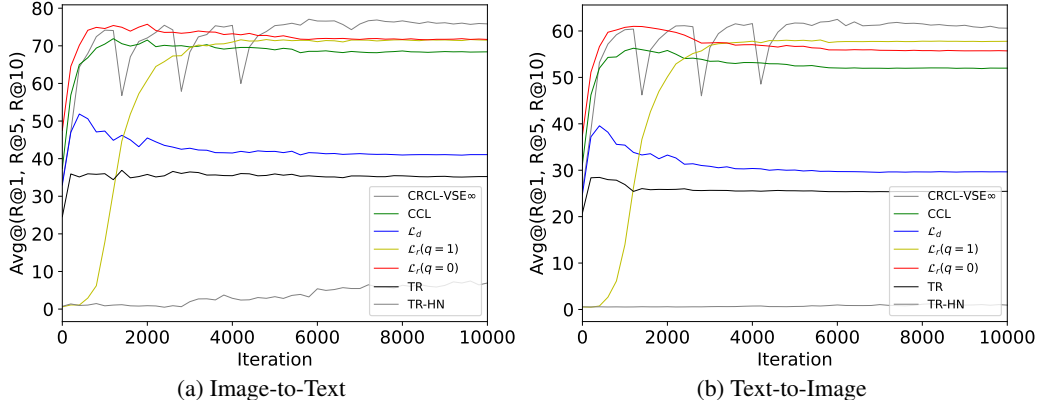


Figure 4: The performance of VSE_∞ with different loss functions.

C.3 More Results under Synthetic Noisy Correspondences

To fully demonstrate the superiority and generalization of the proposed CRCL, we provide more comparison results under different robustness frameworks, including DECL² [19] and BiCro³ [20]. In Table 6, except for the results of BiCro under 20%, 40%, and 60%, all other results are reproduced by us. From the results, our CRCL can significantly improve the robustness of existing methods (e.g., VSE_∞ , SAF, and SGR) and outperform other advanced robust frameworks. It is worth noting that CRCL is also stable and superior in high noise, which shows the effectiveness of our CRCL.

C.4 More Results under Well-annotated Correspondences

In this section, we supplement the experimental results under well-annotated correspondences for a comprehensive and faithful comparison, including 17 state-of-the-art baselines, namely VSRN (ICCV’19) [42], CVSE (ECCV’20) [43], VSE_∞ (CVPR’21) [9], MV-VSE (IJCAI’22) [44]; SCAN (ECCV’18) [8], CAMP (ICCV’19) [45], IMRAM (CVPR’20) [46], GSMN (CVPR’20) [47], SGRAF (AAAI’21) [4], NCR (NeurIPS’21) [12], DECL (ACM MM’22) [19], CGMN (TOMM’22) [48], URDA (TMM’22) [49], CMCAN (AAAI’22) [50], NAAF (CVPR’22) [51], CCR&CCS (WACV’23) [52], RCL (TPAMI’23) [20], and BiCro (CVPR’23) [23]. From the experimental results in Table 7, our CRCL achieves competitive results, which demonstrates the ability and potential of CRCL to handle well-correspondence scenarios.

D Related works

D.1 Image-Text Matching

Image-text matching methods mainly focus on learning latent visual-semantic relevance/similarities as the evidence for cross-modal retrieval [7, 8, 4, 9, 50, 53, 54, 55, 56, 57]. These approaches could be roughly classified into global- and local-level methods. To be specific, most global-level methods [7, 42, 9, 57] project images and texts into a shared global space, wherein cross-modal similarities could be computed [7, 9]. For example, Faghri et al. [7] proposed a triplet ranking

²<https://github.com/QinYang79/DECL>

³<https://github.com/xu5zhao/BiCro>

Table 6: Performance comparison (R@K(%) and rSum) of image-text retrieval on Flickr30K and MS-COCO 1K. The highest scores are shown in **bold**.

		Flickr30K							MS-COCO 1K						
		Image → Text			Text → Image										
Noise	Methods	R@1	R@5	R@10	R@1	R@5	R@10	rSum	R@1	R@5	R@10	R@1	R@5	R@10	rSum
20%	SAF	51.8	79.5	88.3	38.1	66.8	76.6	401.1	41.0	78.4	89.4	38.2	74.0	85.5	406.5
	SGR	61.2	84.3	91.5	44.5	72.1	80.2	433.8	49.1	83.8	92.7	42.5	77.7	88.2	434.0
	VSE ∞	69.0	89.2	94.8	48.8	76.3	83.8	461.9	73.5	93.3	97.0	57.4	86.5	92.8	500.5
	DECL-SAF	73.1	93.0	96.2	57.0	82.0	88.4	489.7	77.2	95.9	98.4	61.6	89.0	95.3	517.4
	DECL-SGR	75.4	93.2	96.2	56.8	81.7	88.4	491.7	76.9	95.3	98.2	61.3	89.0	95.1	515.8
	BiCro-SAF	77.0	93.3	97.5	57.2	82.3	89.1	496.4	74.5	95.0	98.2	60.7	89.0	95.0	512.4
	BiCro-SGR	76.5	93.1	97.4	58.1	82.4	88.5	496.0	75.7	95.1	98.1	60.5	88.6	94.7	512.7
	CRCL-VSE∞	74.8	92.8	96.5	55.1	81.8	88.7	489.7	76.2	95.5	98.6	61.3	89.7	95.6	516.9
	CRCL-SAF	74.7	93.7	97.7	57.9	82.8	89.2	496.0	78.5	95.7	98.5	63.1	89.9	95.5	521.2
	CRCL-SGR	75.8	94.6	97.6	59.1	84.0	90.1	501.2	78.9	95.7	98.3	63.6	90.3	95.7	522.5
40%	SAF	34.3	65.6	78.4	30.1	58.0	68.5	334.9	36.0	74.4	87.0	33.7	69.4	82.5	383.0
	SGR	47.2	76.4	83.2	34.5	60.3	70.5	372.1	43.9	78.3	89.3	37.0	72.8	85.1	406.4
	VSE ∞	30.2	58.3	70.2	22.3	49.6	62.7	293.3	53.3	84.3	92.1	31.4	63.8	75.0	399.9
	DECL-SAF	72.2	91.4	95.6	54.0	79.4	86.4	479.0	75.8	95.0	98.1	60.3	88.7	94.9	512.8
	DECL-SGR	72.4	92.2	96.5	54.5	80.1	87.1	482.8	75.9	95.3	98.2	60.2	88.3	94.8	512.7
	BiCro-SAF	72.5	91.7	95.3	53.6	79.0	86.4	478.5	75.2	95.0	97.9	59.4	87.9	94.3	509.7
	BiCro-SGR	72.8	91.5	94.6	54.7	79.0	86.3	478.9	74.6	94.8	97.7	59.4	87.5	94.0	508.0
	CRCL-VSE∞	71.2	92.6	96.3	53.2	80.4	87.4	481.1	74.4	95.1	98.4	59.5	89.1	95.2	511.7
	CRCL-SAF	74.2	93.8	97.1	57.0	81.8	88.6	492.5	76.4	95.7	98.1	62.1	89.3	95.3	516.9
	CRCL-SGR	75.5	94.0	97.8	57.5	82.6	89.2	496.6	76.8	95.3	98.2	61.9	89.6	95.4	517.2
60%	SAF	28.3	54.5	67.5	22.1	47.3	59.0	278.7	28.2	63.9	79.4	31.1	65.6	80.5	348.7
	SGR	28.7	58.0	71.0	23.8	49.5	60.7	291.7	37.6	73.3	86.3	33.8	68.6	81.7	381.3
	VSE ∞	18.0	44.0	55.7	15.1	38.5	51.8	223.1	33.4	64.8	79.1	26.0	60.1	76.3	339.7
	DECL-SAF	66.4	88.1	93.6	49.8	76.1	84.4	458.4	71.1	93.6	97.3	57.9	86.8	93.8	500.5
	DECL-SGR	68.5	89.9	94.8	50.3	76.7	84.1	464.3	73.2	94.4	97.9	58.2	86.8	93.9	504.4
	BiCro-SAF	67.1	88.3	93.8	48.8	75.2	83.8	457.0	72.5	94.3	97.9	57.7	86.9	93.8	503.1
	BiCro-SGR	68.5	89.1	93.1	48.2	74.7	82.7	456.3	73.4	94.0	97.5	58.0	86.8	93.6	503.3
	CRCL-VSE∞	68.3	89.8	95.9	50.5	77.8	85.3	467.6	72.6	94.1	98.0	57.8	87.7	94.5	504.7
	CRCL-SAF	70.1	90.8	95.7	53.0	79.4	86.9	475.9	74.6	94.5	97.6	59.5	88.3	94.7	509.2
	CRCL-SGR	70.5	91.3	95.6	52.5	79.4	86.8	476.1	74.6	94.6	97.9	59.2	88.0	94.6	508.9
80%	SAF	12.2	32.8	48.4	11.8	30.5	41.5	177.2	24.2	57.5	74.1	24.7	57.1	73.0	310.6
	SGR	13.7	35.1	47.6	12.1	30.9	41.9	181.3	26.7	60.7	75.6	25.3	58.2	72.6	319.1
	VSE ∞	8.1	23.1	34.7	7.4	22.6	31.8	127.7	25.4	55.1	70.6	19.2	50.5	68.0	288.8
	DECL-SAF	56.3	82.1	89.3	38.7	64.7	73.8	404.9	65.9	92.0	96.6	52.9	83.6	91.7	482.7
	DECL-SGR	55.1	79.8	87.2	37.4	63.4	72.9	395.8	65.6	91.6	96.6	52.0	83.0	91.3	480.1
	BiCro-SAF	2.4	9.1	15.8	2.4	8.3	13.7	51.7	39.6	72.6	84.7	22.4	52.8	67.1	368.9
	BiCro-SGR	1.7	8.7	13.7	1.3	5.1	8.9	39.4	31.4	62.0	75.2	30.0	60.7	73.2	332.5
	CRCL-VSE∞	55.3	82.1	89.1	39.7	68.2	77.8	412.2	67.9	92.8	97.1	53.1	84.7	92.5	488.1
	CRCL-SAF	58.4	83.9	90.5	44.1	70.7	79.8	427.4	70.9	92.8	97.1	55.2	85.3	92.9	494.2
	CRCL-SGR	59.2	85.1	91.1	43.6	70.9	80.1	430.0	70.7	92.9	97.1	56.0	85.6	93.1	495.4

loss with hard negatives to learn holistic visual-semantic embeddings for cross-modal retrieval. A Generalized Pooling Operator (GPO) [9] was proposed to adaptively aggregate different features (*e.g.*, region-based and grid-based ones) for better common representations. For the local-level methods, most of them desire to learn the latent fine-grained alignments across modalities for more accurate inference of visual-semantic relevance [8, 4, 50]. Representatively, Lee et al.[8] proposed a Stacked Cross Attention Network model (SCAN) to excavate the full latent alignments by contextualizing the image regions and word tokens for visual-semantic similarity inference. Diao et al. [4] proposed a Similarity Graph Reasoning and Attention Filtration model (SGRAF) for accurate cross-modal similarity inference by using a graph convolutional neural network for fine-grained alignments and an attention mechanism for representative alignments. Moreover, Zhang et al. [50] proposed a novel Cross-Modal Confidence-Aware Network to combine the confidence of matched region-word pairs with local semantic similarities for a more accurate visual-semantic relevance measurement. HREM [57] could explicitly capture both fragment-level relations within modality and instance-level relations across different modalities, leading to better retrieval performance. Pan et.al [56] propose a Cross-modal Hard Aligning Network (CHAN) to comprehensively exploit the most relevant region-word pairs and eliminate all other alignments, achieving better retrieval accuracy and efficiency. However, the aforementioned methods rely heavily on well-aligned image-text pairs while ignoring the inevitable noisy correspondences in data [12, 19], which will mislead the cross-modal learning and lead to performance corruption.

Table 7: Performance comparison (R@K(%) and rSum) of image-text retrieval on Flickr30K and MS-COCO 1K. The highest scores are shown in **bold**. * means global-level method.

Methods	Flickr30K							MS-COCO 1K							
	Image → Text			Text → Image				rSum	Image → Text			Text → Image			
	R@1	R@5	R@10	R@1	R@5	R@10	R@1		R@5	R@10	R@1	R@5	R@10	rSum	
VSRN*	71.3	90.6	96.0	54.7	81.8	88.2	482.6	76.2	94.8	98.2	62.8	89.7	95.1	516.8	
CVSE*	70.5	88.0	92.7	54.7	82.2	88.6	476.7	69.2	93.3	97.5	55.7	86.9	93.8	496.4	
VSE _∞ *	76.5	94.2	97.7	56.4	83.4	89.9	498.1	78.5	96.0	98.7	61.7	90.3	95.6	520.8	
MV-VSE*	79.0	94.9	97.7	59.1	84.6	90.6	505.9	78.7	95.7	98.7	62.7	90.4	95.7	521.9	
SCAN	67.4	90.3	95.8	48.6	77.7	85.2	465.0	72.7	94.8	98.4	58.8	88.4	94.8	507.9	
CAMP	68.1	89.7	95.2	51.5	77.1	85.3	466.9	72.3	94.8	98.3	58.5	87.9	95.0	506.8	
IMRAM	74.1	93.0	96.6	53.9	79.4	87.2	484.2	76.7	95.6	98.5	61.7	89.1	95.0	516.6	
GSMN	76.4	94.3	97.3	57.4	82.3	89.0	496.7	78.4	96.4	98.6	63.3	90.1	95.7	522.5	
SGRAF	77.8	94.1	97.4	58.5	83.0	88.8	499.6	79.6	96.2	98.5	63.2	90.7	96.1	524.3	
NCR	77.3	94.0	97.5	59.6	84.4	89.9	502.7	78.7	95.8	98.5	63.3	90.4	95.8	522.5	
DECL	79.8	94.9	97.4	59.5	83.9	89.5	505.0	79.1	96.3	98.7	63.3	90.1	95.6	523.1	
CGMN	77.9	93.8	96.8	59.9	85.1	90.6	504.1	76.8	95.4	98.3	63.8	90.7	95.7	520.7	
UARDA	77.8	95.0	97.6	57.8	82.9	89.2	500.3	77.8	95.0	97.6	57.8	82.9	89.2	500.3	
CMCAN	79.5	95.6	97.6	60.9	84.3	89.9	507.8	78.6	96.5	98.9	63.9	90.7	96.2	524.8	
NAAF	78.3	94.1	97.7	58.9	83.3	89.0	501.3	78.9	96.0	98.7	63.1	91.4	96.5	524.6	
CCR&CCS	79.3	95.2	98.0	59.8	83.6	88.8	504.7	80.2	96.8	98.7	64.3	90.6	95.8	526.4	
RCL	79.9	96.1	97.8	61.1	85.4	90.3	510.6	80.4	96.4	98.7	64.3	90.8	96.0	526.6	
BiCro	80.7	94.3	97.6	59.8	83.8	89.7	505.9	78.3	95.8	98.5	62.7	90.0	95.7	521.0	
CRCL	78.5	95.5	98.0	62.3	86.5	91.7	512.5	80.7	96.5	98.6	65.1	91.2	96.1	528.2	

D.2 Learning with Noisy Labels

Since the lack of well-annotated data in many real-world applications [26, 58, 59, 60, 31, 61, 62, 12], learning with incomplete/noisy supervision information is becoming more and more popular in recent years. In this section, we briefly review a few families of these methods against noisy labels: **1) Robust losses** aims to improve the robustness of loss functions to prevent models from overfitting on noisy labels [26, 33, 63, 64, 32, 59]. **2) Sample selection** [21, 65] mainly exploits the memorization effect of DNNs [25] to divide/select the corrupted samples from datasets, and then conduct different training strategies for clean and noisy data. **3) Correction Approaches**[66, 67, 68] attempt to correct the wrong supervision information (*e.g.*, labels or losses) for robust training through some ingenious mechanisms. Different from the aforementioned unimodal category-based methods, learning with noisy correspondence focuses on the noisy annotations existing across different modalities instead of classes [12, 19]. That is to say, noisy correspondences are instance-level noise instead of class-level noise, which is more challenging [12, 19]. To tackle this challenge, Huang et al. [12] first proposed a novel Noisy Correspondence Rectifier (NCR) to rectify the noisy correspondences with co-teaching. By introducing evidential deep learning into image-text matching, Qin et al. [19] proposed a general Deep Evidential Cross-modal Learning framework (DECL) to improve the robustness against noisy correspondences. Some recent works [20, 23] try to predict correspondence labels to recast the margin of triplet ranking loss [7] as a soft margin to further improve robustness like NCR, *e.g.*, cross-modal meta learning [20] and similarity-based consistency learning [23]. In addition to image-text matching, other fields are also troubled by NC, such as partially view-aligned clustering [13, 14, 15, 16], video-text retrieval [17], visible-infrared person re-identification [18]. In this paper, we mainly focus on the NC problem in image-text matching and try to address this from both robust loss function and correspondence correction.